doi:10.1016/S0022-2836(02)01094-X available online at http://www.idealibrary.com on IDEAL® J. Mol. Biol. (2002) 324, 429–442

JMB

Conservation of Helical Structure Contributes to Functional Metal Ion Interactions in the Catalytic Domain of Ribonuclease P RNA

Nicholas M. Kaye, Nathan H. Zahler, Eric L. Christian and Michael E. Harris*

Center for RNA Molecular Biology, and Department of Molecular Biology and Microbiology, Case Western Reserve University School of Medicine, 10900 Euclid Ave Cleveland, OH 44106, USA

Like protein enzymes, catalytic RNAs contain conserved structure motifs important for function. A universal feature of the catalytic domain of ribonuclease P RNA is a bulged-helix motif within the P1–P4 helix junction. Here, we show that changes in bulged nucleotide identity and position within helix P4 affect both catalysis and substrate binding, while a subset of the mutations resulted only in catalytic defects. We find that the proximity of the bulge to sites of metal ion coordination in P4 is important for catalysis; moving the bulge distal to these sites and deleting it had similarly large effects, while moving it proximal to these sites had only a moderate effect on catalysis. To test whether the effects of the mutations are linked to metal ion interactions, we used terbium-dependent cleavage of the phosphate backbone to probe metal ion-binding sites in the wild-type and mutant ribozymes. We detect cleavages at specific sites within the catalytic domain, including helix P4 and J3/4, which have previously been shown to participate directly in metal ion interactions. Mutations introduced into P4 cause local changes in the terbium cleavage pattern due to alternate metal ion-binding configurations with the helix. In addition, a bulge deletion mutation results in a 100-fold decrease in the single turnover cleavage rate constant at saturating magnesium levels, and a reduced affinity for magnesium ions important for catalysis. In light of the alternate terbium cleavage pattern in P4 caused by bulge deletion, this decreased ability to utilize magnesium ions for catalysis appears to be due to localized structural changes in the ribozyme's catalytic core that weaken metal ion interactions in P4 and J3/4. The information reported here, therefore, provides evidence that the universal conservation of the P4 structure is based in part on optimization of metal ion interactions important for catalysis.

*Corresponding author

Keywords: ribozyme; metal ion; terbium; RNA structure; ribonuclease P

Introduction

Many essential cellular processes depend on the function of ribonucleoproteins (RNPs) such as the ribosome, spliceosome and numerous smaller RNP enzymes. These RNPs contain distinct species of RNA molecules that, like their protein counterparts, have phylogenetically conserved sequences and structures that are central to biological function. However, in contrast to our broad understanding of the roles of protein structural motifs, our knowledge of the functional roles of conserved RNA structural motifs is only beginning to emerge. Here, we examine the role of a bulged-helix motif in the catalytic core of the RNA subunit of the RNP enzyme ribonuclease P (RNase P), and provide evidence that its function is to facilitate binding of metal ions important for catalysis.

RNase P is an endonuclease involved in the maturation of tRNA, 4.5 S RNA and other cellular RNAs.[1,2] In bacteria, the enzyme is composed of a ~400 nucleotide RNA and a smaller, ~120 amino acid protein subunit. It is now well established that bacterial[3] and some archeal RNase P RNAs[4] can bind substrates and catalyze phosphodiester bond hydrolysis, demonstrating that the active site

Abbreviations used: RNP, ribonucleoprotein.

E-mail address of the corresponding author: meh2@pop.cwru.edu

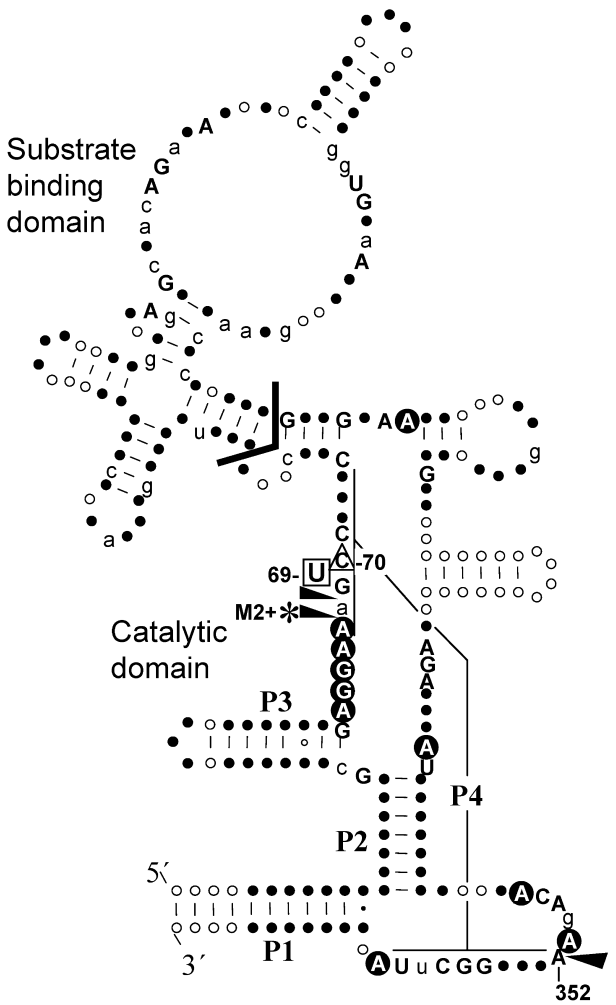

Figure 1. Consensus secondary structure of bacterial RNase P RNA.[12] Capital letters indicate universally conserved nucleotides, lower case letters are 80% conserved, small filled circles represent nucleotide positions that are 100% conserved, and small open circles indicate nucleotide positions that are 80% conserved. The conserved bulged uridine (U69 in *E. coli* RNase P RNA) in helix P4 is boxed; C70, where mutation engenders a change in metal ion usage for catalysis, is indicated by a triangle. Nucleotides that are circled are sites where analog substitution interferes with ribozyme catalysis and arrows indicate phosphorothioate-sensitive positions. An asterisk highlights the site of metal ion coordination at A67.

of the enzyme is composed of RNA. Although eukaryotes and archea contain additional protein subunits,[5–7] their RNase P RNAs retain an essential conserved core of sequences and secondary structures[8–10] that are likely to be directly involved in catalytic function. Although much is known about the enzyme's folding dynamics, structure, and recognition of the substrate,[1,2] the specific roles of most conserved structural and functional elements of the ribozyme are not well understood.

A distinguishing feature of RNase P RNA structure[8–12] and the related RNP enzyme, RNase MRP,[13–16] is a four-way helix junction encompassing helices P1 through P4 (P1–P4; Figure 1). Biochemical and mutational studies, in addition to phylogenetic comparative sequence analysis, have confirmed that P1–P4 is a functionally important element of the ribozyme's catalytic core.[11,17–21] For example, several adjacent regions of structure form short-range (<3 Å) cross-links with nucleotides proximal to the substrate cleavage site.[22–24] Additionally, the majority of the functional groups that are known to be important for ribozyme catalysis are located within P1–P4.[21,25,26] Among these important ribozyme functional groups are phosphate oxygen atoms at positions A67, G68 and A352 in *Escherichia coli* RNase P RNA, where phosphorothioate substitutions lower the cleavage rate constant by three to four orders of magnitude[20,25] (Figure 1). Within helix P4, at A67, rescue of the deleterious effects of these phosphorothioate modifications by "thiophilic" metal ions has provided evidence that magnesium (Mg^{2+}) interactions in P4 are crucial for catalytic function.[17,20,25] Additionally, a C to U point mutation at position 70 (C70U) results in a dramatic increase in the ability of the ribozyme to use calcium (Ca^{2+}) as a catalytic metal ion.[27]

Lying between C70 and A67 in helix P4 is a universally conserved single bulged uridine residue, U69.[8–12] The proximity of the conserved bulge to residues associated with metal ion binding, together with the demonstration that the bulged geometry influences cobalt hexamine binding in a model P4 system,[28] strongly suggests that helix structure may play an important role in Mg^{2+} interactions important for catalysis. The present study tests the role of this conserved element of P4 structure by examining the effects of mutations that alter the identity and position of the U69 bulge on binding, catalysis and metal ion interactions. The results are consistent with the view that the bulged U69 residue is conserved, in part, due to its role in maintaining helical geometry important for metal ion interactions. These observations support the emerging principle that asymmetric bulged-helix motifs are a common theme for essential metal ion interactions in functional RNA structure.

Results

Effects of bulge modification and mutation on ribozyme catalysis

To understand the role of the bulged residue in P4, we first tested whether sugar–phosphate backbone functional groups at the U69 position contributed to ribozyme catalysis. 2′H, 2′O–CH_3, and R_P and S_P phosphorothioate modifications were incorporated at U69 within a self-cleaving (*cis*) ribozyme–substrate conjugate system previously used for identification and analysis of functional groups involved in catalysis.[20] As shown in Table 1, deletion or methylation of the 2′

Table 1. Effects of modification and mutation in helix P4 on catalysis and binding

Ribozyme	*Cis*[a] reaction		*Trans*[a] reaction			
	k_c (min^{-1})	k_c^{wt}/k_c^{mut}	k_c (min^{-1})	k_c^{wt}/k_c^{mut}	K_d (nM)	K_d^{mut}/K_d^{wt}
PT50	0.6 ± 0.3	1				
PT50(U69dU)[b]	0.3 ± 0.1	2				
PT50(U69mU)[b]	0.3 ± 0.2	2				
PT50(U69R_P)[b,c]	0.09 ± 0.04	7				
PT50(U69S_P)[b,c]	0.8 ± 0.4	0.8				
RNase P RNA			0.26 ± 0.03	1	1.7 ± 0.5	1
U69A	0.12 ± 0.01	4	0.062 ± 0.004	5	4 ± 3	2.4
U69g	0.05 ± 0.03	12	0.0034 ± 0.0004	76	73 ± 25	43
U69C	0.03 ± 0.01	20	0.0056 ± 0.0004	46	3 ± 2	1.8
U69Δ	0.012 ± 0.004	50	0.0056 ± 0.0007	46	7 ± 2	4
U70			0.0054 ± 0.0009	48	181 ± 63	106
U69Δ–U68			0.015 ± 0.005	17	65 ± 35	38
U69Δ–U70			0.0036 ± 0.0009	72	5 ± 2	2.9

[a] *Cis* refers to self-cleavage by PT50 or modified PT50 ribozymes. Standard *cis* conditions are trace [5′-^{32}P]ribozyme, 3 M NaCl, 50 mM Pipes, 25 mM $MgCl_2$ (pH 5.5) at 50 °C. *Trans* refers to the native reaction where substrate is not tethered to the ribozyme. Standard *trans* conditions are 4 nM [5′-^{32}P]pre-tRNA^{Asp}, 1.5 μM ribozyme, 1 M NaCl, 50 mM Pipes, 25 mM $MgCl_2$ (pH 6) at 37 °C.
[b] dU refers to removal of the 2′OH at position 69. Similarly, mU refers to addition of a 2′O–CH_3, R_P refers to substitution of the pro-R_P non-bridging phosphate oxygen with sulfur, and S_P refers to substitution of the pro-S_P non-bridging phosphate oxygen with sulfur.
[c] From Christian et al.[20]

hydroxyl and an S_P phosphorothioate substitution affected catalytic rate less than twofold. In contrast, a modest effect (sevenfold) was observed for the R_P phosphorothioate modification, as noted previously.[20] The sevenfold defect is not rescuable by thiophilic metal ions (data not shown), and may be due to changes to the helical geometry in P4 that effect activity. Thus, the backbone modifications tested only confer relatively small defects to ribozyme activity.

Next, we tested the importance of the base identity at U69 by analyzing the binding and catalytic behavior of a series of mutant ribozymes. The mutants were tested both in the context of the *cis*-cleaving ribozyme system as well as the native, *trans*-cleaving reaction. As shown in Table 1, the self-cleaving system produced results similar to the native system. Using the *trans* system we find that, in contrast to the small effect of phosphodiester backbone modification, mutation of the uridine base to G or C resulted in relatively large (greater than ~50-fold) decreases in the cleavage rate constant, k_c (Figure 2 and Table 1). Interpretation of the effects of U69G and U69C mutations are complicated by the fact that these mutations can result in alternative pairing interactions within P4 (see below, Figure 6). However, the U69A mutation, which is not expected to alter the pattern of base-pairing in P4, resulted in only a fivefold reduction in k_c. This result was unanticipated, since the functional groups presented by A and U differ significantly, and, since uridine is universally conserved at this position. It was possible that U69A displayed a small catalytic defect because the role of the bulge was to facilitate interactions with the *E. coli* protein subunit, C5. Although C5 stimulated the reaction under low salt conditions, holoenzymes containing a U69 mutant RNA displayed catalytic defects of the same magnitude as the RNA alone (data not shown). In addition, the apparent dissociation constant for substrate binding, K_d^{app}, increased substantially only for the U69G mutant (Figure 2 and Table 1). We conclude from these data that the presence of a bulged residue at U69 is primarily important for catalysis, but that the individual functional groups on the nucleotide base and phosphodiester backbone contribute relatively little to function.

Given the relatively small catalytic defect engendered by altering base functional groups, but large effect with mutants that may cause miss-pairings, we examined the role of helix geometry in ribozyme function with a series of mutant ribozymes that altered the size or position of the internal bulge (Table 1 and Figure 6). Increasing the size of the bulge from one nucleotide to two (U70) resulted in a 48-fold decrease in k_c and a 106-fold increase in K_d^{app}. Deleting the bulge (U69Δ) caused a 46-fold decrease in k_c and a small, fourfold increase in K_d^{app}. Thus, the size of the bulge is important for catalysis and substrate binding; however, the simple presence of the bulge is important primarily for catalysis. Moving the bulge one nucleotide in the 3′ direction (U69Δ–U70) resulted in a significant, 72-fold catalytic defect, and only a threefold increase in K_d^{app}. In contrast, relocating the bulge one nucleotide in the 5′ direction (U69Δ–U68) resulted in a relatively moderate (17-fold) reduction in k_c and a 38-fold increase in K_d^{app}. Since moving the bulge residue closer to the metal-binding sites at A65–A67[20,29] had a smaller effect on catalysis than movement of the bulge away from the site of Mg^{2+} interaction, these results suggest a link between the bulge structure and functional metal ion interactions. Furthermore, the idea that the role of the uridine bulge lies primarily in catalysis is supported, once again, by the fact that while several mutants result in

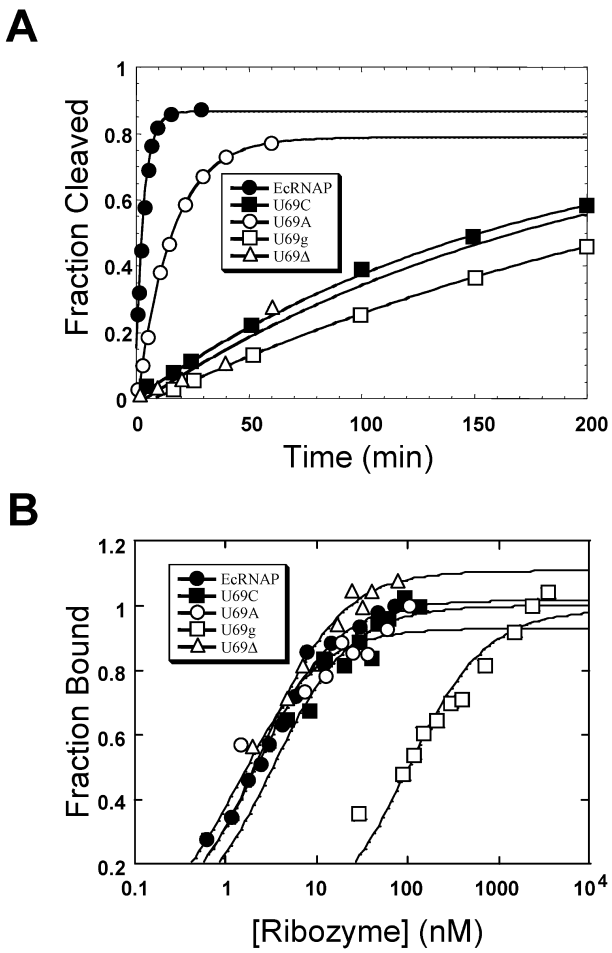

Figure 2. Effect of U69 deletion and mutation on catalysis and substrate binding. (A) Determination of the single turnover rate constant for native *E. coli* RNase P RNA and mutants with alterations at U69. Reactions contained 4 nM [5′-^{32}P]pre-tRNA^{Asp}, 1 M NaCl, 50 mM Pipes (pH 6), 15 mM $MgCl_2$ at 37 °C. Plots of product accumulation *versus* time are shown. The rate constants for catalysis given in Table 1 were obtained by fitting the data to a single exponential function (equation (1)). (B) Effect of U69 mutation on substrate binding. Reaction conditions were 1 M NH_4OAc, 10 mM $CaCl_2$, 50 mM Pipes (pH 6) at 37 °C. Bound and unbound substrates were separated by native gel electrophoresis[77,78] and the fraction bound is plotted as a function of enzyme concentration. The data are fit to a single-binding isotherm (equation (2)) and the resulting dissociation constants are reported in Table 1.

substrate-binding defects, a subset display only small-binding defects, yet relatively large catalytic defects.

Analysis of potential metal ion-binding sites by terbium (Tb^{3+}) cleavage

Phosphorothioate inhibition and subsequent rescue with thiophilic metal ions such as manganese (Mn^{2+}) has been used to measure the affinity of a bound metal ion at the A67 phosphate of RNase P RNA.[29] Therefore, we initially sought to directly measure potential changes in metal ion affinity of the rescuable A67 metal ion in the context of a phosphorothioate-substituted, bulge deletion mutant. However, under the experimental conditions used here, we found this doubly modified ribozyme to be completely inactive, even after two weeks of incubation in the presence of Mn^{2+} (data not shown).

As an alternative, we reasoned that despite some limitations, the trivalent form of the lanthanide metal ion Tb^{3+} could be used to assess changes in structure and metal binding properties induced by mutation or repositioning the U69 bulge. Tb^{3+} cleavage of the RNA backbone is a broadly applied method for examining sites of metal ion interactions and changes in RNA structure.[30–33] Unlike Mg^{2+}, Tb^{3+} catalyzes cleavage of the RNA backbone at physiological pH due to a lower pK_a (pK_a^{Mg} = 11; pK_a^{Tb} = 7.9). Thus, the pattern of Tb^{3+} cleavage of native RNase P RNA can provide insight into potential Mg^{2+}-binding sites in P1–P4 and throughout the molecule, and that of mutants can reveal information concerning local or global mis-folding, since such metal ion interactions are likely to be sensitive to changes in tertiary structure.

As shown in Figure 3(A), in the presence of 15 mM Mg^{2+} to ensure proper folding, a specific pattern of cleavage was observed for the native *E. coli* RNase P ribozyme from 0.04 mM to 0.1 mM Tb^{3+}. At higher concentrations of Tb^{3+}, there is a proportional increase in the intensity of cleavage until, at the highest concentration, there is detectable cleavage at nearly all nucleotides. In order to maximize cleavages that result from site-specific binding, we performed subsequent mapping experiments at low concentrations of Tb^{3+} (40–80 μM), and high (1 M) concentration of monovalent ions, which is expected to compete effectively with non-specific or diffuse Tb^{3+} interactions.[34,35] Under these conditions, we find that cleavages occur primarily within regions of non-Watson–Crick structure and at the base of helices (Figures 3 and 4). In the catalytic domain of the ribozyme, significant cleavage occurred at nucleotides in J3/4, J5/6, J5/15, J18/2, and at the ends of helix P4. In the substrate-binding domain, cleavages occur in L8, P10, and J11/12. Although it was difficult to map cleavage sites precisely in and around helices P13 and P14, inspection of the gels did not show a significant number of cleavages in this region.

To highlight positions that most likely represent bona fide Mg^{2+} coordination sites, we identified Tb^{3+} cleavages that were effectively competed by increasing concentrations of Mg^{2+} (Figure 3(A) and (B)). At 150 mM Mg^{2+}, the Tb^{3+} cleavage pattern of RNase P RNA is nearly identical with the pattern at 15 mM Mg^{2+}, but higher concentrations of Tb^{3+} are required to attain an equivalent level of cleavage. Notably, sites in P10 appear less sensitive to Mg^{2+} concentration, and may therefore represent Tb^{3+}-binding sites not normally filled by Mg^{2+}

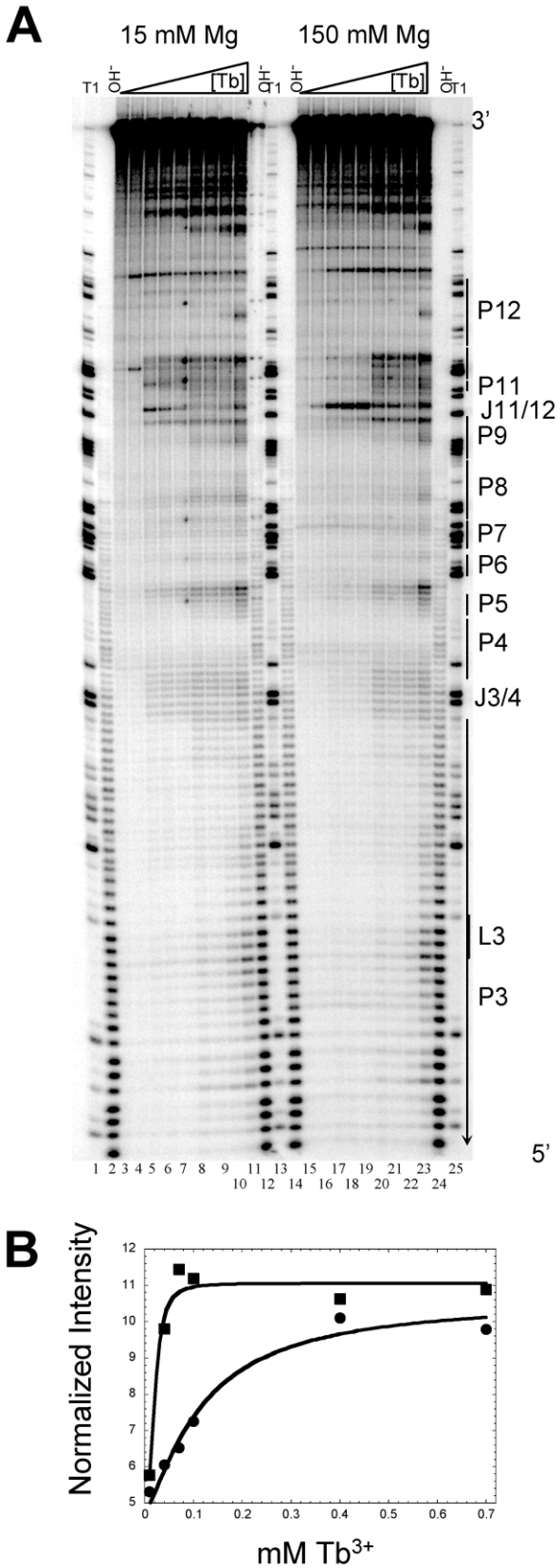

Figure 3. Analysis of Tb^{3+} induced cleavage of *E. coli* RNase P RNA. (A) Tb^{3+} cleavage pattern at 15 mM or 150 mM Mg^{2+}. Lanes 1, 13, and 25 are RNase T_1 digestion ladders. Lanes 2, 12, 14, and 24 show alkaline hydrolysis ladders of RNase P RNA. Lanes 3–11 and 15–23 show the Tb^{3+} cleavage pattern of RNase P RNA at 0, 0.01, 0.04, 0.07, 0.1, 0.4, 0.7, 1, and 5 mM Tb^{3+}, respectively. Lanes 3–11 were performed at 15 mM Mg^{2+} and lanes 15–23 were performed at 150 mM Mg^{2+}. The corresponding elements of RNase P secondary structure are indicated on the right of the gel. (B) Mg^{2+} competition of Tb^{3+} cleavage in helix P4. Plot of the Tb^{3+} titration for the normalized intensity of nucleotides 61–67 at 15 (squares) or 150 mM $MgCl_2$ (circles). Data are fit to a single-binding isotherm (equation (2)), and the resulting apparent affinities are reported in the text.

(Figure 3(A)). Tb^{3+} competition is quantified in Figure 3(B) with a plot of the normalized intensity of cleavages at A61–A67 *versus* Tb^{3+} concentration for 15 mM and 150 mM Mg^{2+}. The concentration of Tb^{3+} required for half-maximal cleavage intensity increases fivefold from ~0.02 mM at 15 mM Mg^{2+} to ~0.1 mM at 150 mM Mg^{2+}. The ability of Mg^{2+} to compete for Tb^{3+}-binding sites in and adjacent to P4 suggests that Tb^{3+}-binding sites overlap significantly with sites of Mg^{2+} interaction. Also, we observe that low concentrations (ca 50 mM) of Tb^{3+} inhibit RNase P ribozyme catalysis, supporting the hypothesis that Tb^{3+} binding competes for functional metal ion interactions (data not shown). It is also formally possible that increased Mg^{2+} concentrations change the tertiary structure of RNase P RNA in ways that weaken Tb^{3+} binding in an indirect manner. However, we consider this possibility unlikely as 15 mM Mg^{2+} is well in excess of that required for complete folding.[36–39] In sum, the Tb^{3+} cleavage data located a number of putative divalent metal ion-binding sites in RNase P RNA, including positions within helix P4 and J3/4 where divalent metal-binding sites had been previously identified (A62–A67).

Effects of U69 mutation on the Tb^{3+} cleavage pattern in J3/4–P4

Next, we reasoned that Tb^{3+} cleavage could be used to assess changes in structure and metal binding properties induced by mutating or repositioning the U69 bulge. Changes in sensitivity to Tb^{3+} cleavage could occur for several reasons, including elimination of a specific metal-binding site, or by changing local backbone geometry such that it is less susceptible to attack even in the presence of a bound metal ion. Furthermore, it may be that not all metal ion binding sites result in RNA strand cleavage. Nevertheless, it is likely that the effect of mutation on a large, but not necessarily complete, subset of metal binding sites can be examined by monitoring Tb^{3+} cleavage.

As shown in Figures 5 and 6, we found that mutation or repositioning of the uridine bulge results in localized changes in the Tb^{3+} cleavage pattern limited to the cluster of strong cleavages at nucleotides 61–69, adjacent to the site of mutation. Because the global Tb^{3+} cleavage pattern remains the same for all the mutants, we conclude that

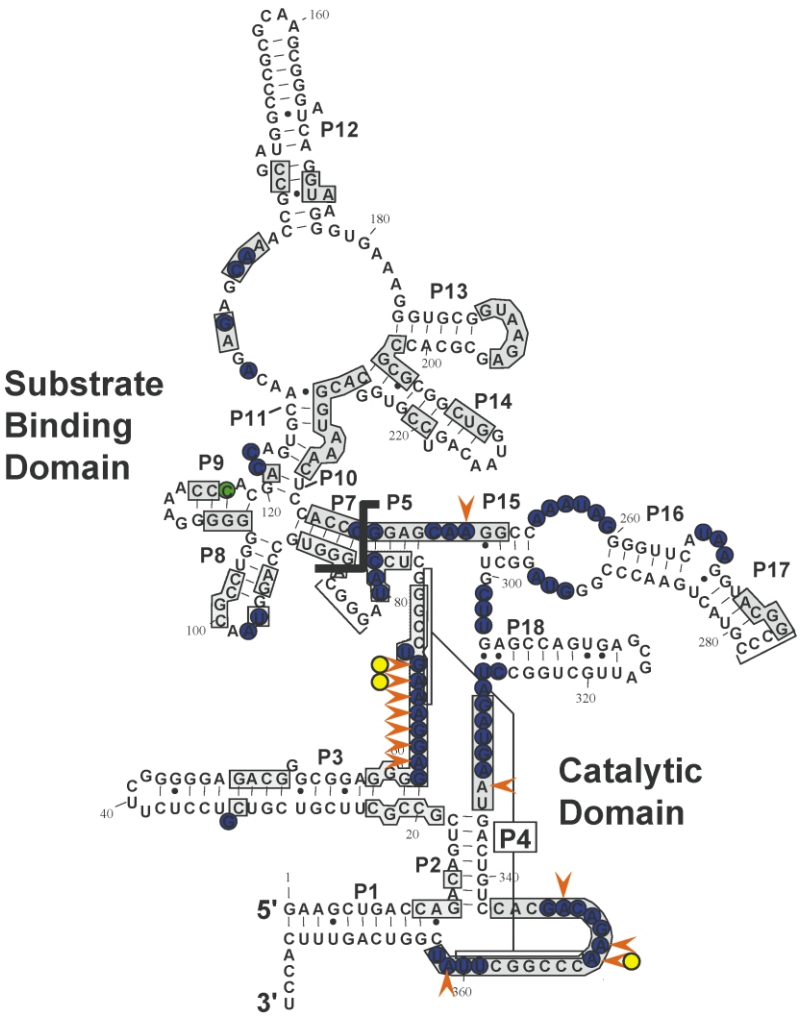

Figure 4. Location of Tb^{3+} cleavage sites in *E. coli* RNase P. Blue circles denote nucleotides sensitive to Tb^{3+} cleavage. Gray boxes indicate nucleotide positions protected from hydroxide radical cleavage.[37] Red arrows indicate individual nucleotide positions where nucleotide analog substitution interferes with catalytic activity.[21,26] Yellow circles indicate sites of phosphorothioate inhibition.

none of the mutations cause a global miss-folding or unfolding of the ribozyme. Furthermore, the size and position of the bulge influenced the pattern of cleavages in P4 and J3/4, verifying that our approach is a sensitive monitor of local structural changes induced by the mutations. For U69G and C, there is a reduction in the cleavage intensity at nucleotides 68 and 69, whereas U69A displays a cleavage pattern essentially identical to the native ribozyme, as expected. Like U69A, U70 displays strong cleavages at the same nucleotides as the wild-type ribozyme; however, the intensity of cleavage is increased. This may reflect a more open conformation of the helix engendered by the two-nucleotide bulge that allows metal ions to bind in P4, but in a geometry that is not ideal for catalysis. When the bulge is deleted in U69Δ, even fewer Tb^{3+} cleavages are detected then with U69G or C, with a reduction in intensity at positions 66, 67, 68, and 69. The remaining major cleavages are in the single-stranded J3/4 region. Since the helix no longer contains a bulge, the major groove of P4 should no longer be widened, and therefore may be less able to accommodate metal ions distal to the base of the helix. U69Δ–U70 has reduced Tb^{3+} cleavage at positions 66, 67, 68, and 69, similar to U69Δ. This is consistent with a more regular helical geometry at the base of helix P4. Although the number and position of Tb^{3+} cleavages in U69Δ–U68 is the same as in U69Δ–U70, cleavages are enhanced at nucleotides 63, 64, 65, and 66, consistent of an opening of the base of helix P4 that allows metal ions to be accommodated. Together, the Tb^{3+} cleavage patterns of the mutant ribozymes shows that alterations in helix geometry perturb metal ion-binding properties of helix P4 either through enhancement or reduction of cleavages. The exception is U69A, which has both a Tb^{3+} cleavage pattern nearly identical with the native ribozyme and retains near wild-type activity.

Effect of U69 deletion on metal ion interactions important for catalysis

To more directly quantify the effects of U69 mutation on metal ion interactions important for catalysis, we determined the dependence of k_c on Mg^{2+} concentration using wild-type RNase P RNA and the U69 deletion mutant. We chose to examine U69Δ because it has a large (46-fold) catalytic defect, a small (fourfold) binding defect (Table 1), and a large metal ion-binding defect at A67 as

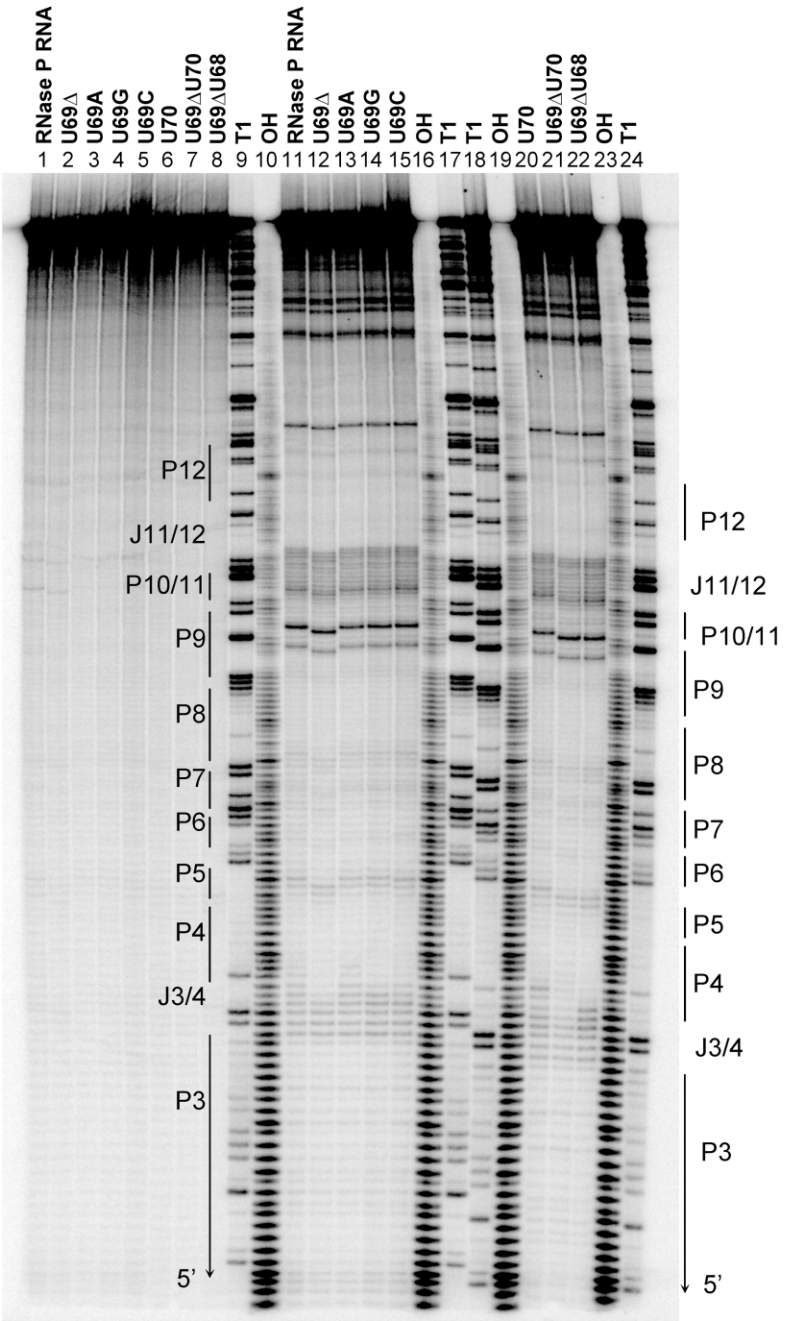

Figure 5. Effects of U69 mutation on Tb^{3+} cleavage. Lanes 9, 17, 18 and 24 are T_1 digestion standards and lanes 10, 16, 19 and 23 are alkaline hydrolysis ladders. Lanes 1–8 are RNAs that were mock treated and lanes 11–15 and 20–22 show digestion products of (5′-^{32}P)labeled ribozymes incubated in the presence of 80 μM Tb^{3+}. Digestion reactions were performed at 15 mM $MgCl_2$ as described in Materials and Methods. The corresponding elements of RNase P secondary structure are indicated on the right of the gel. Native RNase P RNA, U69Δ, U69A, U69G and U69C have an additional two guanosine residues at their 5′ ends to facilitate T7 transcription and so migrate correspondingly slower than U70, U69Δ–U68 and U69Δ–U70 RNAs.

determined by Tb^{3+} cleavage. Importantly, the mutation is not expected to engender mis-pairing in P4. Analysis of metal titration experiments using catalysis as a read out is complicated by the fact that metal ions contribute to RNase P RNA folding and substrate binding as well as to catalysis.[40–43] To ensure proper folding and substrate binding at low Mg^{2+} levels, we pre-incubated enzyme and substrate in a background of 10 mM $CaCl_2$.[41,44,45] The k_c value was then measured at increasing Mg^{2+} concentrations (0–300 mM). To control for changes in substrate affinity at different metal ion concentrations, single turnover rate constants were determined at saturating enzyme concentration, where the observed rate constant reflects the rate of cleavage of the bound substrate.

Figure 7 shows a plot of the observed rate constant as a function of Mg^{2+} concentration for the native RNase P RNA and U69Δ. The rate constant at saturating Mg^{2+} (k_c^{Mg}), apparent Mg^{2+} affinity ($K_{1/2}^{Mg}$), and cooperativity (Hill coefficient, n_H) of binding was measured by fitting the data to a non-linear form of the Hill equation (equation (3); Figure 7). Under the conditions utilized, the cleavage rate constant for the native ribozyme saturates with respect to Mg^{2+} concentration at $k_c^{Mg} \sim 4\ min^{-1}$. Catalysis is cooperatively dependent on Mg^{2+} concentration ($n_H = 2.2$), and $K_{1/2}^{Mg} = 150$ mM. These results are consistent with

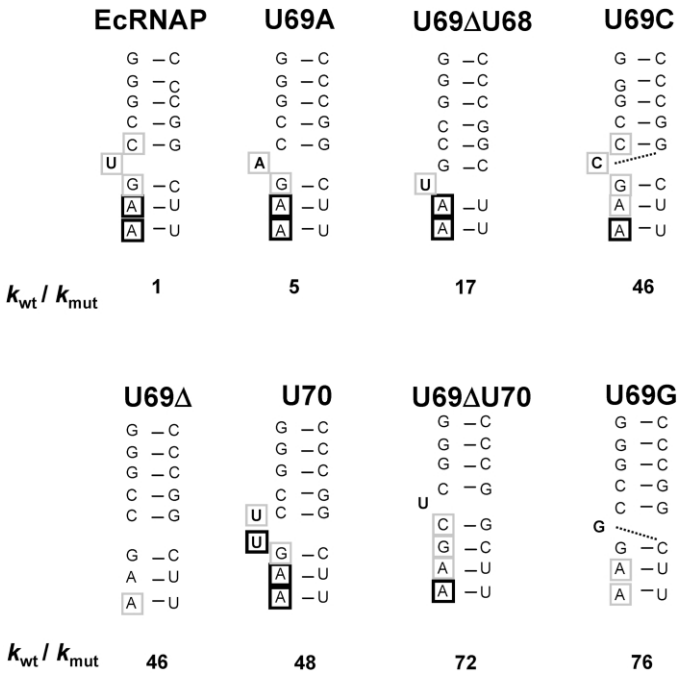

Figure 6. Summary of Tb^{3+} cleavages within helix P4 of native RNase P RNA and U69 mutant RNAs. The relative cleavage rate constants shown in Table 1 are depicted below the proposed secondary structure for wild-type helix P4 and those of the mutant ribozymes. Nucleotides susceptible to Tb^{3+} cleavage are boxed. Black and gray boxes indicate strong and weak cleavage sites, respectively. The relative intensity was quantified as described in Materials and Methods.

previous metal titration studies that also reflect a requirement for binding of multiple, interdependent metal ions.[43,44,46–48] Comparison of the metal titration data for U69Δ with that obtained for the native enzyme reveals four important differences (Figure 7): (1) at saturating concentrations of Mg^{2+}, U69Δ has a 100-fold lower catalytic rate constant ($0.041 \pm (0.007)\ min^{-1}$ compared to the wild-type ribozyme $3.92 \pm (0.02)\ min^{-1}$); (2) the mutant shows a lower degree of cooperativity for stimulation by Mg^{2+} as reflected in the observation that n_H was reduced by 0.7 units to 1.5; (3) the overall affinity for metal ions was weakened in the mutant, as shown by a corresponding ~twofold increase in $K_{1/2}^{Mg}$ to 285 mM; and (4) k_c for U69Δ is actually larger than for the native ribozyme in Ca^{2+} alone. These results indicate that a simple alteration of helix geometry in the catalytic core, while having only small local effects on ribozyme structure, has significant effects on the affinity and selectivity of metal ion interactions required for catalysis.

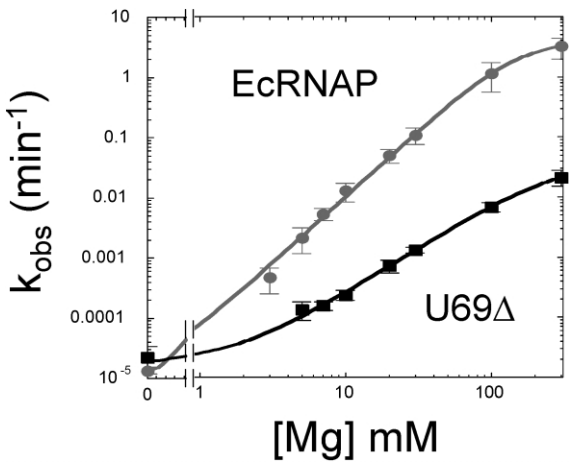

Figure 7. Comparison of the metal ion dependence of the native ribozyme and the U69Δ mutant. The single turnover reaction rate for the native (circles) and U69Δ (squares) ribozymes is plotted as a function of Mg^{2+} concentration (0–300 mM Mg^{2+}). Error bars represent one standard deviation from the mean of at least three experiments. Data are fit to a non-linear form of the Hill equation (equation (3)) and the resulting parameters, $K_{1/2}$, k_{max}, and n_H are reported in the text.

Discussion

Extensive comparative sequence analysis of RNase P RNAs from all three phylogenetic domains has provided a detailed perspective on the variability and conservation of secondary and tertiary structure.[9–12,49,50] Like other essential cellular RNAs, RNase P RNAs throughout phylogeny retain a conserved core important for function. The observation that "minimal" RNase P RNAs constructed to contain only core sequence and structure are catalytic underscores this view.[51,52]

Importantly, RNase P RNA contains characteristic sequence and structure motifs that make it distinct from all other non-coding functional RNAs. While crystallographic and functional group modification experiments have provided important insights into the basis for nucleotide conservation in other large ribozymes, most notably the group I intron from Tetrahymena,[53–57] the functional basis that underlies conservation of sequence and structure in RNase P RNA is poorly understood.

Many of the conserved residues in RNase P RNA are located in the P1–P4 multi-helix junction, a

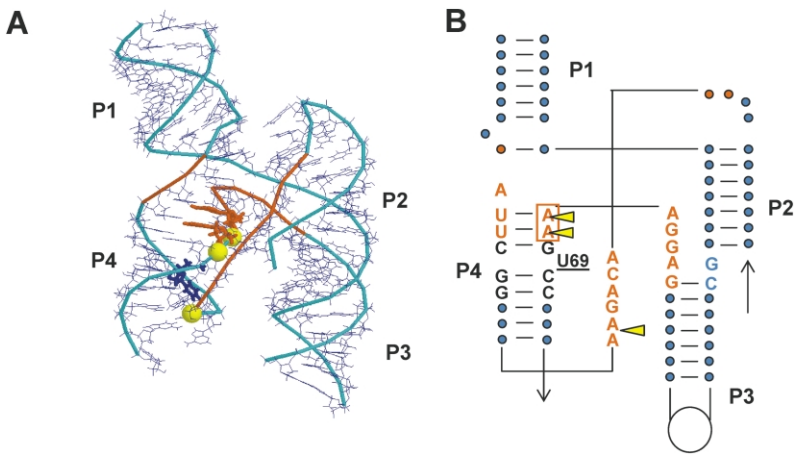

Figure 8. Regions of metal ion interaction in the P1–P4 four-way helix junction. (A) Detail from the model structure of the P1–P4 four-way helix junction.[79,80] Regions of sensitivity to Tb^{3+} cleavage are shown in red, the location of U69, A67 and A66 are indicated in dark blue and red, respectively. The locations of phosphate groups that are sensitive to phosphorothioate modification are shown as yellow spheres. (B) Secondary structure diagram of P1–P4 from (A). The structure is redrawn to reflect the helix stacking arrangement and path of the phosphodiester backbone within the available structure models. Universally conserved nucleotides are indicated by letters. The regions of Tb^{3+} cleavage are indicated in red. Sites of sensitivity to phosphorothioate modification are indicated by yellow arrows.

central feature of the ribozyme's conserved core (Figure 8), including the universally conserved bulged uridine residue located adjacent to residues in P4 and J3/4 known to be involved in critical divalent metal ion interactions. Additionally, P4 is proximal to the scissile bond in low resolution structure models of the ribozyme–substrate complex. For these reasons, P4 has been hypothesized to make up a portion of the active site of the ribozyme. Thus, in this study we examined the role in ribozyme function of the universally conserved bulged uridine in helix P4.

Backbone functional group substitutions and changes in the identity and position of the bulged residue in P4 were tested for their effects on catalytic activity. In sum, the kinetic and themodynamic behavior of the mutants show that the identity of the bulged residue was not critical; however, changes in the position of the bulge within P4 resulted in relatively large defects in ribozyme activity. Importantly, moving the bulge closer to the sites of metal ion interactions at A67 and in J3/4 could be better accommodated than deletion or moving the bulge distal to J3/4. Given the proximity of the bulge to the A67 metal ion-binding site (see Figure 8) and the known association between distortions in helix geometry and major groove metal ion interactions,[58] we hypothesized that the bulged-helix geometry of P4 facilitates functional metal ion interactions.

The sensitivity of metal ion binding to helix structure has also been suggested by the observation that a C70U mutation altered the metal ion specificity of the ribozyme.[27] This same mutation results in a relocation of the bulge as determined by NMR analysis of an isolated mutant P4 helix.[28] In the case of the model P4, the C to U change resulted in a repositioning of a bound cobalt hexamine ion within the major groove.[28] A similar change in helix geometry is likely to distort the metal ion-binding interactions that occur in P4 in the context of the entire ribozyme.

In the folded ribozyme, helix P4 is thought to be positioned in the interior of the ribozyme, and inspection of the secondary structures shows that both ends of P4 are located in complex multi-helix junctions (see Figures 1 and 8). Given its central location, changes in P4 geometry could be translated to other elements in the tertiary structure. Thus, it is feasible that the mutations that alter P4 geometry could perturb catalytic function and substrate binding by disrupting distal or local structure. To test whether mutations in P4 resulted in any structural perturbations, and to learn more about metal ion interactions in P1–P4 in general, we undertook a series of metal ion cleavage studies using Tb^{3+}. In addition to information about potential metal ion binding-sites, the structure dependence of metal ion induced cleavage has been used to gain additional information regarding alteration of RNA tertiary structure.[45,59,60] In this manner, lead-induced cleavage has been previously used to demonstrate mis-folding engendered by mutation in the catalytic domain of RNase P RNA.[61,62]

We find that the sites of Tb^{3+} cleavage in the native ribozyme occur throughout the structure in regions expected to form complex non-Watson–Crick interactions (Figure 4) and importantly, the solvent inaccessible regions of the ribozyme as determined by hydroxyl radical cleavage.[37] Hydroxide radicals generated by metal ion coordination can cleave the solvent accessible surface of a folded RNA, and protection from cleavage is generally interpreted as reflecting involvement in higher-order RNA structure.[37,39,42,63–65] As shown in Figure 4, there is significant overlap between sites of Tb^{3+} cleavage and sites protected from hydroxyl radical cleavage. The correspondence is particularly good in several regions within the catalytic domain. In particular, the Tb^{3+} cleavages in the P1–P4 multi-helix junction, including J3/4 (G61–A65), P4 (A66–U69; U359–U362) and J2/4 (G346–A352), occur at nucleotides that show

strong protection from solvent attack by hydroxide radical.

Additionally, there is significant overlap between the Tb^{3+} mapping data and information from modification interference studies that identified functional groups within the catalytic domain important for the substrate cleavage reaction[21,25,26] (Figure 4). The nucleotide positions that are protected from solvent and are sensitive to Tb^{3+} cleavage and nucleotide analog substitution are located in J3/4 (A62–A65), P4 (A66–G68; A361), J5/15 (A249), and J2/4 (A347, A351, A352). The clustering of Tb^{3+} cleavage sites around important functional groups in J3/4 and P4 is consistent with the use of multiple metal ions to bring together the complex network of single-stranded and helical structures required to form the ribozyme active site.[29]

The observation that a particular nucleotide is susceptible to cleavage does not necessarily imply a direct role in coordination, but only that the residue is proximal to a bound Tb^{3+} ion. Multiple conformational states of the RNA, or breathing of the helix could allow Tb^{3+} ions to remain proximal to nucleotides for sufficient time to allow backbone cleavage at various positions in P4. On the other hand, within P4 and J3/4, there is evidence that the sites of Tb^{3+} cleavage occur at nucleotides with functional groups directly involved in metal ion binding (Figure 8). Thus, while Tb^{3+} cleavage does not directly delineate specific metal ion interactions at these positions, the extent of Tb^{3+} cleavage is a reasonable sensor of whether mutations alter the general metal ion-binding environment of P1–P4.

Importantly, we found that although several of the mutations had significant defects in catalytic rate, none of the mutations in P4 engendered substantial changes in the global pattern of Tb^{3+} cleavage. The interpretation that the mutations in P4 only engender localized perturbation of ribozyme structure is supported further by the fact that several mutations with relatively large catalytic defects (i.e. U69C, U69Δ, and U69Δ–U70) retained the ability to bind substrate with near native affinity. It is important to note, however, that changes in structure that do not affect Tb^{3+} cleavage will be missed in this analysis. It is difficult to know with precision how great a change in structure is necessary to result in a detectable change in Tb^{3+} cleavage. Previous application of Pb^{2+} cleavage in *E. coli* RNase P RNA showed that specific deletions of phylogenetically variable structure elements produced large changes in cleavage patterns relative to the native ribozyme, indicating alterations in the overall tertiary structures of the mutant RNAs.[59] Additionally, it has been shown that individual mutations in the J18/2 region of the catalytic domain, with effects on function comparable to those reported here, were found to cause disruption of the pattern of Pb^{2+} cleavage.[61] Thus, the consistency of the Tb^{3+} cleavage pattern of the mutants with that of the native ribozyme described here provides evidence that the basis of the functional defects observed is due to relatively local changes in ribozyme structure.

To test whether deletion of the bulge in P4 affects metal ion interactions important for catalysis, we compared the Mg^{2+} dependence of the catalytic activity of the U69Δ ribozyme with that of native RNase P RNA. Remarkably, this simple mutation, which has very little effect on substrate affinity, results in several significant changes in the divalent metal ion dependence of the cleavage reaction. First, the maximal rate constant for catalysis of the U69Δ ribozyme is 100-fold lower than that of the native enzyme at saturating concentrations of Mg^{2+}. This indicates that even with all potential Mg^{2+}-binding sites occupied, the geometry of the ribozyme active site is intrinsically different. Because substrate binding is essentially unaffected by this mutation, and, since the Tb^{3+} cleavage pattern of the U69Δ RNA only differs from the native ribozyme within the P4 helix, we conclude that local changes in structure near the metal ion-binding sites in P4 are responsible for the catalytic defect. Second, the mutant ribozyme shows weakened affinity for catalytic metal ion interactions relative to the native RNase P RNA. Although these data alone do not distinguish between Mg ions that interact directly with the scissile bond and those that interact elsewhere in the RNA, they are nonetheless essential for attaining the transition state. Moreover, because these studies were performed in 10 mM Ca^{2+}, it is likely that most of the "non-catalytic" metal ion-binding sites required for folding and substrate binding are filled. Third, the cooperativity coefficient is reduced by nearly 1 unit, consistent with the loss of a single metal ion or class of metal ions important for catalysis. An intriguing hypothesis is that the metal ion lost may be at A67, as seen from the Tb^{3+} cleavage data. Fourth, in the presence of Ca^{2+} alone, the k_c value is actually larger for U69Δ than for the native ribozyme. This shows that P4 plays a critical role in determining the metal ion utilization properties of RNase P RNA, consistent with the observation that a C70U mutation alters the utilization of metal ions by the ribozyme. In sum, we provide evidence for the reasons behind the conservation of bulge structure within the active site of RNase P. Conservation seems to be maintained, at one level, for the purpose of preventing mismatched base-pair formation within helix P4. This, in turn, provides for an optimal bulge position that can allow helix P4 geometry to accommodate metal ions that are important for function of the ribozyme.

Association of a bulged-helix motif with metal ion binding is clearly not unique to RNase P RNA. Several recent structural studies underscore the importance of bulged-helix motifs in metal ion interactions. For example, structural analysis of the Leadzyme shows that this catalytic RNA features an internal loop in which a bulged purine

base stack twists away from the helical stem, and that this structure is important for accommodating a metal ion in the major groove.[66] Additionally, the bulged structure of the HIV-1 *trans*-activation response region depends on metal ion interactions. One metal ion, crucial to the loop conformation, binds directly to three phosphate groups in the major groove.[67] Also, the crystal structure of helix II of the *Xenopus laevis* 5 S rRNA includes two calcium ions bound in the major groove adjacent to a single bulged cytosine residue. The conformation of this residue is essential for these metal interactions, since an alternative structure with the C interacting within the helix was not found to contain metals.[68]

It is also important to note that bulged-helix motifs associated with divalent metal ion interactions are also found in the conserved cores of the other large ribozymes, in helix P7 and domain V of the self-splicing group I and group II ribozymes, respectively.[69,70] Like helix P4 in the RNase P ribozyme, P7 and domain V are highly conserved and are central to catalytic function. Both P7 and domain V have been shown to bind divalent metal ions at, or near internal bulge motifs.[31,71,72] An asymmetric bulged-helix similar to domain V also forms between snRNAs U2 and U6 in the pre-mRNA spliceosome,[73,74] whose general chemical mechanism is identical with that of group II intron splicing. Like its counterparts in the large ribozymes, the asymmetric bulged-helix within U6 is highly conserved, sensitive to mutation, and has recently been shown to be involved in divalent metal ion interactions important for enzymatic activity.[75] Thus, while the catalytic centers of RNase P, group I and group II introns, and the spliceosome are obviously structurally and functionally distinct, they nevertheless appear to have converged upon a common strategy for obtaining function: utilization of an asymmetric bulged-helix linked to metal ion binding as a structural element important for catalytic activity.

Materials and Methods

Analysis of ribozyme activity

Mutant ribozymes were generated by PCR mutagenesis[76] and the methodology for determining single turnover rate constants and substrate binding affinities were as described.[19,22,77]. *Cis* cleavage reactions were performed as described. *Trans* cleavage reactions were performed as follows. A 12 μl pre-tRNA^{Asp} substrate mix (8 nM [5-^{32}P]pre-tRNA^{ASP}, 1 M NaCl, 50 mM Pipes (pH 6), $MgCl_2$ varied between experiments) and a 10 μl enzyme mix (3 μM enzyme, 1 M NaCl, 50 mM Pipes (pH 6), $MgCl_2$ varied between experiments) were pre-incubated (without $MgCl_2$) at 95 °C for three minutes and 50 °C for two minutes. $MgCl_2$ was added, and the mixtures were further incubated at 50 °C for 40 minutes and 37 °C for 30 minutes. Then 10 μl of substrate was mixed with the 10 μl enzyme mix (substrate = 4 nM, enzyme = 1.5 μM) and 2 μl aliquots were removed at predetermined intervals and quenched with at least twice the final Mg^{2+} concentration of EDTA. For very long reactions, 30 μl of mineral oil were added after eight hours to minimize evaporation. The 2 μl of the quenched reaction products were separated on 7 M urea − 6% (w/v) polyacrylamide gels. Dried gels were quantified using a Molecular Dynamics phosphorimager system and ONE-D scan software, and plotted using KaleidaGraph (Synergy Software) graphing software. Data were fit to the single exponential function of equation (1):

$$\text{Fraction cleaved} = A + B\,e^{-kt} \quad (1)$$

where A is the extent of the reaction, B is the amplitude of the exponential, k is the observed cleavage rate constant, and t is time.

Analysis of substrate binding

To measure the affinity of pre-tRNA^{Asp} for wild-type and mutant forms of the RNase P ribozyme, a native polyacrylamide gel-shift assay was utilized, modified from that previously described.[78] A total of 6 μl of diluted enzyme stocks were added into 12 Eppendorf tubes at four times their final reaction concentration. The enzyme dilutions were then diluted twofold by addition of 6 μl of 2 × reaction buffer such that the final (1 ×) buffer conditions (10 mM Pipes (pH 6.0) at 37 °C, 25 mM $CaCl_2$, 1 M NH_4OAc, 5% (v/v) glycerol) and 2 × ribozyme were in the tubes. A substrate master mix was generated with volume sufficient for three binding reactions (468 μl). The master mix contained 2 × [5′-^{32}P]pre-tRNA^{Asp} and 1 × reaction buffer as described above. The concentration of pre-tRNA^{Asp} was maintained at 0.1 of the lowest ribozyme concentration, or lower. Enzyme and substrate were then folded by heating to 50 °C for 50 minutes and then incubating at 37 °C for 30 minutes. Formation of the enzyme–substrate complex (E·S) was initiated by adding 12 μl of substrate master mix to the 12 μl of ribozyme mix and allowed to equilibrate for 10–15 minutes. Then 3 μl of the reaction were loaded onto native 7% polyacrylamide–0.2% bis-gels while running at 37 °C. Typically, gels were run for three hours to obtain adequate separation between E·S and free substrate.

The data was quantified using a Molecular Dynamics 445Si phosphorimager and ONE-Dscan (Scanalytics, Inc.) software. Data was then plotted using KaleidaGraph (Synergy Software) and fit to the single-binding isotherm in equation (2):

$$\text{Fraction Bound} = \frac{F_{max}}{1 + K_d/[\text{Ribozyme}]} \quad (2)$$

where F_{max} = the maximal fraction of substrate shifted, K_d is the dissociation constant between the ribozyme and substrate, and [Ribozyme] is the ribozyme concentrations used in the experiment.

Tb^{3+} cleavage

An enzyme stock was made by combining 2.5 μl of 4 × reaction buffer (4 M NaCl, 200 mM Pipes (pH 6)), 1.5 μl of water, 2 μl of 2.5 μM unlabeled enzyme, and 1 μl of [5′-^{32}P]labeled ribozyme (75,000 cpm/μl, stored in 0.01% (v/v) Nonidet-P40). RNA was renatured by heating to 85 °C for two minutes, and then cooling to 50 °C. After one minute, 1 μl of an appropriate 10 × $MgCl_2$ stock was added, followed by incubation at 50 °C for ten minutes and 37 °C for 20 minutes. To initiate

Tb^{3+} cleavage reaction, 8 μl of the ribozyme solution was added to 2 μl of a 5× $TbCl_3$ stock freshly dissolved in water. The final reaction volume was 10 μl with reaction conditions of 1 M NaCl, 50 mM Pipes (pH 6) at 37 °C, 0.5 μM enzyme, Mg^{2+} and the appropriate Tb^{3+} concentration. Reactions were incubated at 37 °C for 45 minutes. Reactions were stopped with 20 μl of a solution containing 15 μl of formamide load buffer supplemented with EDTA at twice the final Tb^{3+} and Mg^{2+} concentrations. Then 6 μl of the quenched reaction were resolved using 7 M urea–10% or 15% polyacrylamide gels.

The extent of Tb^{3+} cleavage was quantified using a Molecular Dynamics phosphorimager system and ONE-Dscan software. Band intensity was normalized by dividing the counts in a given band by the total number of counts in its lane both for no Tb^{3+} and Tb^{3+} treated reactions. Then the normalized background was subtracted from the normalized band intensity to give a normalized band intensity of arbitrary units. Strong cleavages were defined as those above 0.8 units and weak cleavages were between 0.4 units and 0.8 units. Visual inspection of the gels corroborated the determination of strong and weak cleavages by this method.

Magnesium titrations

Cleavage reactions in the presence of increasing magnesium concentrations were performed essentially as described for the analysis of ribozyme activity. The only differences were that in addition to the standard conditions of 1 M NaCl, 50 mM Pipes (pH 6), 37 °C, substrate and enzyme mixes contained 10 mM $CaCl_2$. Furthermore, increasing concentrations of 10× $MgCl_2$ were used to make the final magnesium concentrations 0, 3, 5, 7, 10, 20, 30, 100, and 300 mM $MgCl_2$.

k_c was then plotted as a function of Mg^{2+} concentration and fit to the non-linear form of the Hill equation shown in equation (3):

$$k_c = \frac{k_{max}([Mg^{2+}]^{n_H})}{(K_{1/2})^{n_H} + [Mg^{2+}]^{n_H}} \quad (3)$$

where k_c is the rate constant measured at each Mg^{2+} concentration, k_{max} is the cleavage rate constant at saturating Mg^{2+} levels, $[Mg^{2+}]$ is the Mg^{2+} concentration, $K_{1/2}$ is the Mg^{2+} level at which one-half k_{max} is observed, and n_H is the Hill coefficient.

Acknowledgements

We thank Dr Mark Caprara and Dr Tim Nilsen for advice on performing and interpreting the metal ion cleavage studies as well as for comments on the manuscript. We also thank the members of the Harris laboratory for critical reading of the manuscript. This work was supported by NIH grant GM56742 (to M.E.H.). N.M.K. was supported by NIH training grant GM008056.

References

1. Kurz, J. C. & Fierke, C. A. (2000). Ribonuclease P: a ribonucleoprotein enzyme. *Curr. Opin. Chem. Biol.* **4**, 553–558.
2. Frank, D. N. & Pace, N. R. (1998). Ribonuclease P: unity and diversity in a tRNA processing ribozyme. *Annu. Rev. Biochem.* **67**, 153–180.
3. Guerrier-Takada, C., Gardiner, K., Marsh, T., Pace, N. & Altman, S. (1983). The RNA moiety of ribonuclease P is the catalytic subunit of the enzyme. *Cell*, **35**, 849–857.
4. Pannucci, J. A., Haas, E. S., Hall, T. A., Harris, J. K. & Brown, J. W. (1999). RNase P RNAs from some Archaea are catalytically active. *Proc. Natl Acad. Sci. USA*, **96**, 7803–7808.
5. Darr, S. C., Pace, B. & Pace, N. R. (1990). Characterization of ribonuclease P from the archaebacterium *Sulfolobus solfataricus*. *J. Biol. Chem.* **265**, 12927–12932.
6. Brown, J. W. & Haas, E. S. (1995). Ribonuclease P structure and function in Archaea. *Mol. Biol. Rep.* **22**, 131–134.
7. Xiao, S., Houser-Scott, F. & Engelke, D. R. (2001). Eukaryotic ribonuclease P: increased complexity to cope with the nuclear pre-tRNA pathway. *J. Cell. Physiol.* **187**, 11–20.
8. Haas, E. S., Armbruster, D. W., Vucson, B. M., Daniels, C. J. & Brown, J. W. (1996). Comparative analysis of ribonuclease P RNA structure in Archaea. *Nucl. Acids Res.* **24**, 1252–1259.
9. Frank, D. N., Adamidi, C., Ehringer, M. A., Pitulle, C. & Pace, N. R. (2000). Phylogenetic-comparative analysis of the eukaryal ribonuclease P RNA. *RNA*, **6**, 1895–1904.
10. Harris, J. K., Haas, E. S., Williams, D., Frank, D. N. & Brown, J. W. (2001). New insight into RNase P RNA structure from comparative analysis of the archaeal RNA. *RNA*, **7**, 220–232.
11. Chen, J. L. & Pace, N. R. (1997). Identification of the universally conserved core of ribonuclease P RNA. *RNA*, **3**, 557–560.
12. Brown, J. W. (1999). The ribonuclease P database. *Nucl. Acids Res.* **27**, 314.
13. Schmitt, M. E., Bennett, J. L., Dairaghi, D. J. & Clayton, D. A. (1993). Secondary structure of RNase MRP RNA as predicted by phylogenetic comparison. *FASEB J.* **7**, 208–213.
14. Reilly, T. H. & Schmitt, M. E. (1995). The yeast *Saccharomyces cerevisiae*, RNase P/MRP ribonucleoprotein endoribonuclease family. *Mol. Biol. Rep.* **22**, 87–93.
15. Reddy, R. & Shimba, S. (1995). Structural and functional similarities between MRP and RNase P. *Mol. Biol. Rep.* **22**, 81–85.
16. Collins, L. J., Moulton, V. & Penny, D. (2000). Use of RNA secondary structure for studying the evolution of RNase P and RNase MRP. *J. Mol. Evol.* **51**, 194–204.
17. Hardt, W. D., Warnecke, J. M., Erdmann, V. A. & Hartmann, R. K. (1995). Rp-phosphorothioate modifications in RNase P RNA that interfere with tRNA binding. *EMBO J.* **14**, 2935–2944.
18. Frank, D. N., Ellington, A. E. & Pace, N. R. (1996). *In vitro* selection of RNase P RNA reveals optimized catalytic activity in a highly conserved structural domain. *RNA*, **2**, 1179–1188.
19. Siew, D., Zahler, N. H., Cassano, A. G., Strobel, S. A. & Harris, M. E. (1999). Identification of adenosine functional groups involved in substrate binding by the ribonuclease P ribozyme. *Biochemistry*, **38**, 1873–1883.
20. Christian, E. L., Kaye, N. M. & Harris, M. E. (2000). Helix P4 is a divalent metal ion binding site in the

conserved core of the ribonuclease P ribozyme. *RNA*, **6**, 511–519.
21. Kaye, N. M., Christian, E. I. & Harris, M. E. (2002). NAIM and site-specific functional group modification analysis of RNase P RNA: magnesium dependent structure within the conserved P1–P4 multihelix junction contributes to catalysis. *Biochemistry*. In press.
22. Christian, E. L., McPheeters, D. S. & Harris, M. E. (1998). Identification of individual nucleotides in the bacterial ribonuclease P ribozyme adjacent to the pre-tRNA cleavage site by short-range photo- cross-linking. *Biochemistry*, **37**, 17618–17628.
23. Christian, E. L. & Harris, M. E. (1999). The track of the pre-tRNA 5′ leader in the ribonuclease P ribozyme–substrate complex. *Biochemistry*, **38**, 12629–12638.
24. Kufel, J. & Kirsebom, L. A. (1996). Different cleavage sites are aligned differently in the active site of M1 RNA, the catalytic subunit of *Escherichia coli* RNase P. *Proc. Natl Acad. Sci. USA*, **93**, 6085–6090.
25. Harris, M. E. & Pace, N. R. (1995). Identification of phosphates involved in catalysis by the ribozyme RNase P RNA. *RNA*, **1**, 210–218.
26. Kazantsev, A. V. & Pace, N. R. (1998). Identification by modification-interference of purine N-7 and ribose 2′-OH groups critical for catalysis by bacterial ribonuclease P. *RNA*, **4**, 937–947.
27. Frank, D. N. & Pace, N. R. (1997). *In vitro* selection for altered divalent metal specificity in the RNase P RNA. *Proc. Natl Acad. Sci. USA*, **94**, 14355–14360.
28. Schmitz, M. & Tinoco, I., Jr (2000). Solution structure and metal-ion binding of the P4 element from bacterial RNase P RNA. *RNA*, **6**, 1212–1225.
29. Christian, E. L., Kaye, N. M. & Harris, M. E. (2002). Evidence for a polynuclear metal ion binding site in the catalytic domain of ribonuclease P RNA. *EMBO J.* **21**, 2253–2262.
30. Hargittai, M. R. & Musier-Forsyth, K. (2000). Use of terbium as a probe of tRNA tertiary structure and folding. *RNA*, **6**, 1672–1680.
31. Sigel, R. K., Vaidya, A. & Pyle, A. M. (2000). Metal ion binding sites in a group II intron core. *Nature Struct. Biol.* **7**, 1111–1116.
32. Vaidya, A. & Suga, H. (2001). Diverse roles of metal ions in acyl-transferase ribozymes. *Biochemistry*, **40**, 7200–7210.
33. Walter, N. G., Yang, N. & Burke, J. M. (2000). Probing non-selective cation binding in the hairpin ribozyme with Tb(III). *J. Mol. Biol.* **298**, 539–555.
34. Misra, V. K. & Draper, D. E. (1998). On the role of magnesium ions in RNA stability. *Biopolymers*, **48**, 113–135.
35. Bukhman, Y. V. & Draper, D. E. (1997). Affinities and selectivities of divalent cation binding sites within an RNA tertiary structure. *J. Mol. Biol.* **273**, 1020–1031.
36. Zarrinkar, P. P., Wang, J. & Williamson, J. R. (1996). Slow folding kinetics of RNase P RNA. *RNA*, **2**, 564–573.
37. Loria, A. & Pan, T. (1996). Domain structure of the ribozyme from eubacterial ribonuclease P. *RNA*, **2**, 551–563.
38. Pan, T. & Sosnick, T. R. (1997). Intermediates and kinetic traps in the folding of a large ribozyme revealed by circular dichroism and UV absorbance spectroscopies and catalytic activity. *Nature Struct. Biol.* **4**, 931–938.
39. Kent, O., Chaulk, S. G. & MacMillan, A. M. (2000). Kinetic analysis of the M1 RNA folding pathway. *J. Mol. Biol.* **304**, 699–705.
40. Guerrier-Takada, C., Haydock, K., Allen, L. & Altman, S. (1986). Metal ion requirements and other aspects of the reaction catalyzed by M1 RNA, the RNA subunit of ribonuclease P from *Escherichia coli*. *Biochemistry*, **25**, 1509–1515.
41. Smith, D., Burgin, A. B., Haas, E. S. & Pace, N. R. (1992). Influence of metal ions on the ribonuclease P reaction. Distinguishing substrate binding from catalysis. *J. Biol. Chem.* **267**, 2429–2436.
42. Pan, T. (1995). Higher order folding and domain analysis of the ribozyme from *Bacillus subtilis* ribonuclease P. *Biochemistry*, **34**, 902–909.
43. Beebe, J. A., Kurz, J. C. & Fierke, C. A. (1996). Magnesium ions are required by *Bacillus subtilis* ribonuclease P RNA for both binding and cleaving precursor tRNAAsp. *Biochemistry*, **35**, 10493–10505.
44. Brannvall, M. & Kirsebom, L. A. (2001). Metal ion cooperativity in ribozyme cleavage of RNA. *Proc. Natl Acad. Sci. USA*, **98**, 12943–12947.
45. Brannvall, M., Mikkelsen, N. E. & Kirsebom, L. A. (2001). Monitoring the structure of *Escherichia coli* RNase P RNA in the presence of various divalent metal ions. *Nucl. Acids Res.* **29**, 1426–1432.
46. Perreault, J. P. & Altman, S. (1993). Pathway of activation by magnesium ions of substrates for the catalytic subunit of RNase P from *Escherichia coli*. *J. Mol. Biol.* **230**, 750–756.
47. Smith, D. & Pace, N. R. (1993). Multiple magnesium ions in the ribonuclease P reaction mechanism. *Biochemistry*, **32**, 5273–5281.
48. Warnecke, J. M., Held, R., Busch, S. & Hartmann, R. K. (1999). Role of metal ions in the hydrolysis reaction catalyzed by RNase P RNA from *Bacillus subtilis*. *J. Mol. Biol.* **290**, 433–445.
49. James, B. D., Olsen, G. J., Liu, J. S. & Pace, N. R. (1988). The secondary structure of ribonuclease P RNA, the catalytic element of a ribonucleoprotein enzyme. *Cell*, **52**, 19–26.
50. Brown, J. W. *et al.* (1996). Comparative analysis of ribonuclease P RNA using gene sequences from natural microbial populations reveals tertiary structural elements. *Proc. Natl Acad. Sci. USA*, **93**, 3001–3006.
51. Pace, N. R. & Waugh, D. S. (1991). Design of simplified ribonuclease P RNA by phylogenetic comparison. *Methods Enzymol.* **203**, 500–510.
52. Siegel, R. W., Banta, A. B., Haas, E. S., Brown, J. W. & Pace, N. R. (1996). Mycoplasma fermentans simplifies our view of the catalytic core of ribonuclease P RNA. *RNA*, **2**, 452–462.
53. Cate, J. H. *et al.* (1996). Crystal structure of a group I ribozyme domain: principles of RNA packing. *Science*, **273**, 1678–1685.
54. Golden, B. L., Gooding, A. R., Podell, E. R. & Cech, T. R. (1998). A preorganized active site in the crystal structure of the Tetrahymena ribozyme. *Science*, **282**, 259–264.
55. Ortoleva-Donnelly, L., Szewczak, A. A., Gutell, R. R. & Strobel, S. A. (1998). The chemical basis of adenosine conservation throughout the Tetrahymena ribozyme. *RNA*, **4**, 498–519.
56. Strobel, S. A., Ortoleva-Donnelly, L., Ryder, S. P., Cate, J. H. & Moncoeur, E. (1998). Complementary sets of noncanonical base pairs mediate RNA helix packing in the group I intron active site. *Nature Struct. Biol.* **5**, 60–66.

57. Szewczak, A. A., Ortoleva-Donnelly, L., Ryder, S. P., Moncoeur, E. & Strobel, S. A. (1998). A minor groove RNA triple helix within the catalytic core of a group I intron. *Nature Struct. Biol.* **5**, 1037–1042.
58. Cate, J. H. & Doudna, J. A. (1996). Metal-binding sites in the major groove of a large ribozyme domain. *Structure*, **4**, 1221–1229.
59. Zito, K., Huttenhofer, A. & Pace, N. R. (1993). Lead-catalyzed cleavage of ribonuclease P RNA as a probe for integrity of tertiary structure. *Nucl. Acids Res.* **21**, 5916–5920.
60. Ciesiolka, J., Hardt, W. D., Schlegl, J., Erdmann, V. A. & Hartmann, R. K. (1994). Lead-ion-induced cleavage of RNase P RNA. *Eur. J. Biochem.* **219**, 49–56.
61. Hardt, W. D. & Hartmann, R. K. (1996). Mutational analysis of the joining regions flanking helix P18 in *E. coli* RNase P RNA. *J. Mol. Biol.* **259**, 422–433.
62. Heide, C., Pfeiffer, T., Nolan, J. M. & Hartmann, R. K. (1999). Guanosine 2-NH2 groups of *Escherichia coli* RNase P RNA involved in intramolecular tertiary contacts and direct interactions with tRNA. *RNA*, **5**, 102–116.
63. Celander, D. W. & Cech, T. R. (1991). Visualizing the higher order folding of a catalytic RNA molecule. *Science*, **251**, 401–407.
64. Heuer, T. S., Chandry, P. S., Belfort, M., Celander, D. W. & Cech, T. R. (1991). Folding of group I introns from bacteriophage T4 involves internalization of the catalytic core. *Proc. Natl Acad. Sci. USA*, **88**, 11105–11109.
65. Swisher, J., Duarte, C. M., Su, L. J. & Pyle, A. M. (2001). Visualizing the solvent-inaccessible core of a group II intron ribozyme. *EMBO J.* **20**, 2051–2061.
66. Wedekind, J. E. & McKay, D. B. (1999). Crystal structure of a lead-dependent ribozyme revealing metal binding sites relevant to catalysis. *Nature Struct. Biol.* **6**, 261–268.
67. Ippolito, J. A. & Steitz, T. A. (1998). A 1.3 Å resolution crystal structure of the HIV-1 *trans*-activation response region RNA stem reveals a metal ion-dependent bulge conformation. *Proc. Natl Acad. Sci. USA*, **95**, 9819–9824.
68. Xiong, Y. & Sundaralingam, M. (2000). Two crystal forms of helix II of *Xenopus laevis* 5 S rRNA with a cytosine bulge. *RNA*, **6**, 1316–1324.
69. Konforti, B. B. *et al.* (1998). Ribozyme catalysis from the major groove of group II intron domain 5. *Mol. Cell*, **1**, 433–441.
70. Gordon, P. M. & Piccirilli, J. A. (2001). Metal ion coordination by the AGC triad in domain 5 contributes to group II intron catalysis. *Nature Struct. Biol.* **8**, 893–898.
71. Christian, E. L. & Yarus, M. (1993). Metal coordination sites that contribute to structure and catalysis in the group I intron from Tetrahymena. *Biochemistry*, **32**, 4475–4480.
72. Szewczak, A. A., Kosek, A. B., Piccirilli, J. A. & Strobel, S. A. (2002). Identification of an active site ligand for a group I ribozyme catalytic metal ion. *Biochemistry*, **41**, 2516–2525.
73. Madhani, H. D. & Guthrie, C. (1992). A novel base-pairing interaction between U2 and U6 snRNAs suggests a mechanism for the catalytic activation of the spliceosome. *Cell*, **71**, 803–817.
74. Costa, M., Christian, E. L. & Michel, F. (1998). Differential chemical probing of a group II self-splicing intron identifies bases involved in tertiary interactions and supports an alternative secondary structure model of domain V. *RNA*, **4**, 1055–1068.
75. Yean, S. L., Wuenschell, G., Termini, J. & Lin, R. J. (2000). Metal-ion coordination by U6 small nuclear RNA contributes to catalysis in the spliceosome. *Nature*, **408**, 881–884.
76. Dulau, L., Cheyrou, A., Dubourdieu, D. & Aigle, M. (1989). Directed mutagenesis using PCR. *Nucl. Acids Res.* **17**, 2873.
77. Beebe, J. A. & Fierke, C. A. (1994). A kinetic mechanism for cleavage of precursor tRNA(Asp) catalyzed by the RNA component of *Bacillus subtilis* ribonuclease P. *Biochemistry*, **33**, 10294–10304.
78. Hardt, W. D., Schlegl, J., Erdmann, V. A. & Hartmann, R. K. (1993). Gel retardation analysis of *E. coli* M1 RNA–tRNA complexes. *Nucl. Acids Res.* **21**, 3521–3527.
79. Massire, C., Jaeger, L. & Westhof, E. (1998). Derivation of the three-dimensional architecture of bacterial ribonuclease P RNAs from comparative sequence analysis. *J. Mol. Biol.* **279**, 773–793.
80. Chen, J. L., Nolan, J. M., Harris, M. E. & Pace, N. R. (1998). Comparative photocross-linking analysis of the tertiary structures of *Escherichia coli* and *Bacillus subtilis* RNase P RNAs. *EMBO J.* **17**, 1515–1525.

Edited by J. Doudna

(Received 17 June 2002; received in revised form 6 September 2002; accepted 9 September 2002)